Journal of Catalysis 301 (2013) 227–232

Contents lists available at SciVerse ScienceDirect

Journal of Catalysis

journal homepage: www.elsevier.com/locate/jcat

CO oxidation over ZnO films on Pt(1 1 1) at near-atmospheric pressures

Y. Martynova [a], B.-H. Liu [a], M.E. McBriarty [a,b], I.M.N. Groot [a], M.J. Bedzyk [b], S. Shaikhutdinov [a,*], H.-J. Freund [a]

[a] Abteilung Chemische Physik, Fritz-Haber-Institut der Max-Planck-Gesellschaft, Germany
[b] Department of Materials Science and Engineering, Northwestern University, United States

ARTICLE INFO

Article history:
Received 17 January 2013
Revised 20 February 2013
Accepted 20 February 2013
Available online 26 March 2013

Keywords:
CO oxidation
Thin oxide films
Zinc oxide

ABSTRACT

Well-ordered ultrathin ZnO(0 0 0 1) films were grown on Pt(1 1 1) in a layer-by-layer mode. The reactivity of the films as a function of the film thickness and coverage was examined by the CO oxidation reaction at near-atmospheric pressures. At low temperatures (~450 K), CO_2 production is found to be much higher on the films of partial coverage than on dense ZnO(0 0 0 1) films and bare Pt(1 1 1). Under reaction conditions, monolayer islands and an entire monolayer film transform into two-monolayers-thick islands, which dominate the surface of the active catalysts. The results provide an adequate structural model for elucidating the reaction mechanism on the oxide/metal boundary at technologically relevant conditions.

1. Introduction

Thin oxide films grown on metal single crystals are suitable supports for modeling heterogeneous catalysts. Recent studies demonstrated that *ultrathin* films, those with thickness of only a few monolayers, may exhibit interesting catalytic properties which are different from those of thicker films or their bulk counterparts [1,2]. For example, an iron oxide FeO(1 1 1) monolayer (ML) film grown on Pt(1 1 1) shows a higher CO oxidation rate than multi-nanometer-thick iron oxide films or clean Pt(1 1 1) when the reaction takes place at near-atmospheric pressures and low temperatures (~450 K) [3]. Accordingly, the encapsulation of Pt nanoparticles by an FeO layer, which occurs as a result of strong metal-support interaction between Pt and Fe_3O_4(1 1 1), resulted in higher activity as compared to pure Pt particles [4]. A higher reaction rate than on Pt(1 1 1) has been predicted for a 2 ML-thick MgO(1 0 0) film on Ag(1 0 0) [5]. Although CO oxidation follows different reaction mechanisms for these two systems, the important steps include charge transfer from the oxide–metal interface to oxygen which is accompanied by an oxide lattice distortion. It is therefore anticipated that the film thickness may affect the reaction, particularly when charge transfer is the rate-limiting step. If the film thickness does matter, then this allows one to tune the reactivity and selectivity of such an "inverted" catalyst, where an oxide phase is supported by a metal, in contrast to a traditional oxide-supported metal catalyst.

In fact, such ideas have already been put forward, most notably by Vol'kenstein [6] and Schwab [7] (see also a critical review by Slinkin and Fedorovskaya [8]), who developed the so-called electron theory of catalysis based, in essence, on the concept of Schottky barriers. However, in that time, the preparation and atomic scale characterization of thin oxide films was not feasible. Establishing direct relationships between the film thickness and the reactivity requires controllable growth of well-ordered oxide films in a layer-by-layer mode. Furthermore, in order to elucidate the role of the oxide phase in the reaction, it is necessary to compare the reactivity of various metal oxide films on the same support.

Bearing all this in mind and having the above-mentioned FeO(1 1 1)/Pt(1 1 1) system as a benchmark, we addressed here the preparation and reactivity of zinc oxide films on Pt(1 1 1). Note that bulk ZnO has the wurtzite structure which is, when projected to the (0 0 0 1) plane, somewhat similar to FeO(1 1 1). Both structures consist of alternating close-packed layers of oxygen and metal ions. The growth of well-ordered ZnO films was previously reported in the literature using Ag(1 1 1) and Pd(1 1 1) single-crystal substrates. With the help of surface X-ray diffraction and scanning tunneling microscopy (STM), Tusche et al. [9] reported that 2–4 ML-thick ZnO(0 0 0 1) films grown on Ag(1 1 1) are somewhat depolarized. That is the surface-normal displacement of Zn and O atoms is reduced such that the film resembles the co-planar sheets in the hexagonal boron nitride (or graphite) structure. The transition to the bulk wurtzite structure is accompanied by considerable surface roughening. On Pd(1 1 1), Weirum et al. [10] also observed layer-by-layer growth for ZnO films up to at least 5 ML. Low-energy electron diffraction (LEED) and STM results together with density functional theory calculations suggested that the graphite-like structure is thermodynamically the most stable phase over a large range of oxygen chemical potentials, before it converges to the bulk-type wurtzite structure at a film thickness above 4 ML.

* Corresponding author. Fax: +49 30 8413 4105.
E-mail address: shaikhutdinov@fhi-berlin.mpg.de (S. Shaikhutdinov).

0021-9517/$ - see front matter © 2013 Elsevier Inc. All rights reserved.
http://dx.doi.org/10.1016/j.jcat.2013.02.018

Numerous experimental and theoretical studies of ZnO single-crystal surfaces, recently reviewed by Wöll [11], were primarily focused on the polar stability and adsorption properties of ZnO surfaces with respect to methanol synthesis and related reactions which occur on ZnO-based catalysts. CO oxidation has also been studied on ZnO powders and films ([12–15] and references therein). Early results revealed (see survey in Ref. [15]) that the activity of ZnO surfaces strongly depends on the temperature, doping, illumination, and sample preparation. A comparative study on the reactivity of polycrystalline and single-crystal ZnO in CO oxidation by Göpel and co-workers [15] showed that the elementary steps of the catalytic oxidation of CO on both systems can be explained quantitatively on the basis of electronic charge transfer reactions accompanied by band bending. Consequently, it was suggested that the catalytic activity can be enhanced significantly by applying an electric field. These authors also concluded that CO oxidation is a face-specific reaction which occurs only at the non-polar ZnO(10–10) surface.

Weiss and Folman [12] studied CO oxidation activity over ZnO films fabricated on Ag foil by radio-frequency sputtering as a function of the film thickness. The authors found that the elementary constants in the rate equations for CO oxidation depend on the film thickness. Good agreement between experimental results and theory based on the Schottky model together with the rigid band model has been observed. Note, however, that the thinnest films studied in this work were about 20 nm in thickness, and the reaction was carried out at elevated temperatures, that is, 600–650 K.

To continue our previous works on CO oxidation over ultrathin oxide films, we studied here the reactivity of ZnO films on Pt(111) at low temperatures (~450 K) and near-atmospheric pressures. The films were characterized by LEED, Auger electron spectroscopy (AES), temperature-programmed desorption (TPD), and STM. The structure-reactivity relationships suggest the oxide/metal boundary as the most active region under the conditions studied.

2. Experimental

The experiments were performed in two ultrahigh vacuum (UHV) chambers (base pressure below 2×10^{-10} mbar) equipped with LEED, AES (both from Specs), and quadrupole mass spectrometers (QMS, from Hiden) for TPD measurements. One chamber houses a gold-plated high-pressure reaction cell for reactivity studies at atmospheric pressures using a gas chromatograph (GC, from Agilent) for the gas composition analysis. The double-side polished Pt(111) crystal was spot-welded to thin Ta wires for resistive heating. The second chamber is equipped with a STM (Omicron) and has an additional Au-plated cell, separated from the main chamber by the gate valve, for high-pressure treatments to mimic technologically relevant reaction conditions. The Pt(111) crystal is clamped to an Omicron sample holder. In both setups, the sample temperature was measured by a Type K thermocouple spot-welded to the edge of the crystal.

A clean Pt(111) surface was obtained by cycles of Ar^+-sputtering and annealing in UHV and O_2. Zinc was deposited by heating a Zn rod (1 mm in diameter, 99.99%, Goodfellow) to 480–520 K by passing current through a tungsten wire wrapped around the rod. The Zn source is shielded by a metal cylinder having a small orifice (~ 5 mm in diameter) and placed about 2 cm away from a crystal. The deposition flux was controlled via a Type K thermocouple spot-welded to the edge of the Zn rod. The zinc oxide films were prepared by Zn deposition onto clean Pt(111) in 10^{-7} mbar O_2 followed by oxidation at 600 K in 10^{-6}–10^{-5} mbar O_2 for 20 min. For reactivity studies, oxide films were grown on both sides of the crystal.

The reaction gas mixture, consisting of 10 mbar CO and 50 mbar O_2 balanced with He to 1 bar, was dosed at room temperature and circulated with a velocity of about 3 ml min^{-1} for ca. 20 min. Then, the sample was heated to 450 K with a rate of 1 Ks^{-1}, and the reaction was monitored by GC.

STM images shown herein were taken with Pt–Ir tips at bias voltages of 1–2 V and tunneling currents of 0.5–0.7 nA. The images were subjected to a plane correction.

3. Results and discussion

Fig. 1 shows LEED patterns and Auger spectra of the "as-prepared" films with increasing thickness. The surface coverage was measured by CO titration of Pt sites using TPD of CO that desorbs from Pt(111) at 300–500 K (see Fig. S1). For more than one monolayer coverage, the nominal thickness was measured by integrating the 32 amu (O_2) desorption signal during film decomposition at $T > 950$ K (Fig. S2). In addition, the thickness was monitored by AES via attenuation of the Pt-related signals (Fig. S3).

The diffraction spots of ZnO(0001)-(1×1) are aligned with those of Pt(111) and show up together with the surrounding hexagonal spots. The latter can be straightforwardly assigned to a coincident Pt(111)-(6×6) superstructure, similar to that observed on ZnO/Pd(111) [10], that arises due to the mismatch between the lattice constants of ZnO(0001) and Pt(111) (3.25 and 2.78 Å, respectively). Basically, six Pt(111) surface unit cells coincide with five ZnO(0001) cells along the surface lattice directions. The surface ZnO lattice is strained by about 3% versus the bulk lattice. Above 2–3 ML, the films only show a relatively diffuse pattern of ZnO(0001) with a high background intensity. The ZnO-related spots were sometimes streaky in the "tangential" direction, thus indicating the presence of domains slightly misaligned with respect to the metal support underneath.

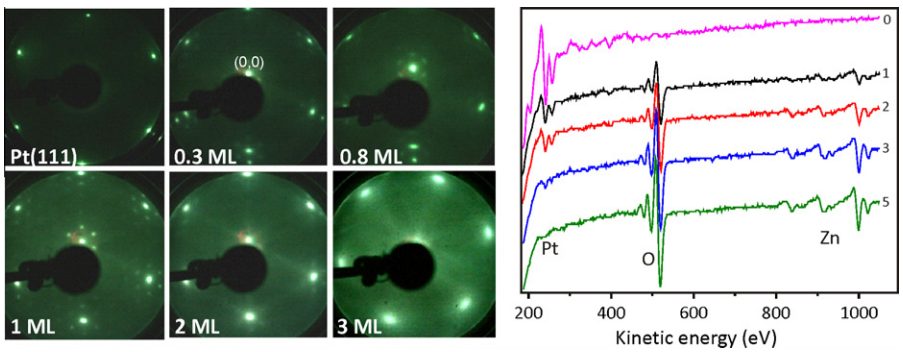

Fig. 1. LEED patterns (at 60 eV, left panel) and Auger spectra (right panel) of ZnO films grown on Pt(111) at the nominal film thicknesses as indicated. Monolayer equivalent (MLE) values are shown to the right of the Auger spectra.

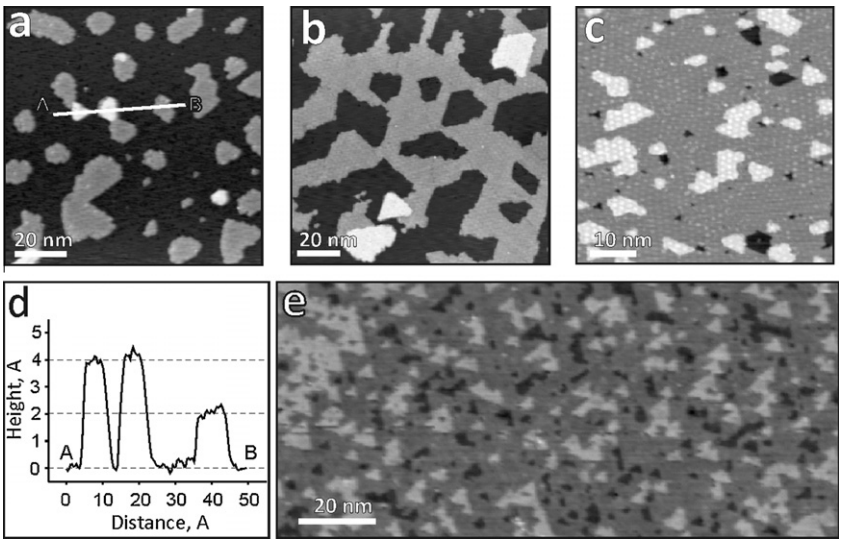

Fig. 2. STM images of the "as-prepared" ZnO films on Pt(1 1 1) at 0.25 (a), 0.55 (b), 1.2 (c) and 4 MLE (e) coverages. (d) Shows a profile scan along the A–B line marked in (a).

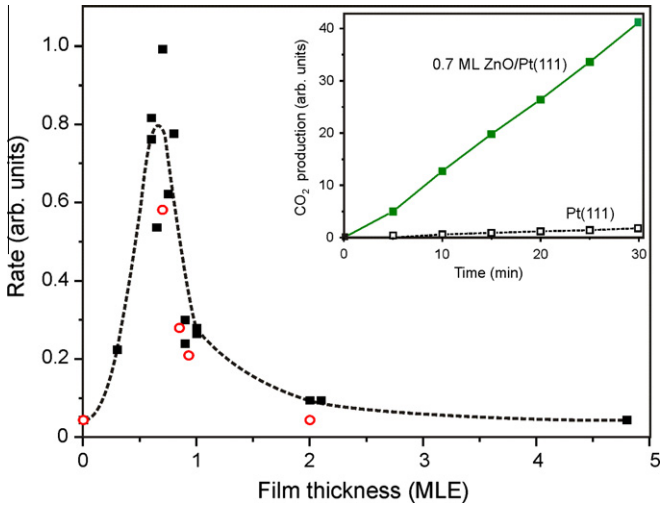

Fig. 3. CO_2 production rate measured over ZnO films on Pt(1 1 1) as a function of the nominal film thickness (in MLE). Solid and open symbols show data for the films prepared using reactive Zn deposition at 85 and 300 K, respectively. Note that for the sub-monolayer films, the film thickness corresponds to the surface coverage as measured by CO titration of Pt(1 1 1). The inset shows kinetic curves for CO_2 production on the pure Pt(1 1 1) and 0.7 ML ZnO(0 0 0 1) film. Reaction conditions: 10 mbar CO + 50 mbar O_2, He balance to 1 bar; 450 K.

To address the morphology of the ZnO films, we performed STM studies in another UHV chamber on similarly prepared samples which were also characterized by LEED and AES. At sub-monolayer coverages, Pt(1 1 1) terraces were randomly covered by two-dimensional islands (Fig. 2a). The height measurements revealed that the islands are predominantly of ~2 Å in apparent height, although a few islands of ~4 Å in height were also observed (see line profile in Fig. 2d). These values correspond to one and two layers of graphite-like ZnO, respectively. (Henceforth, we will refer to the amount of Zn which forms a dense monolayer film as one monolayer equivalent (MLE)). Both mono- and bilayer islands showed Moiré superstructure with a ~17 Å periodicity (Fig. 2c), which is consistent with the Pt(1 1 1)-(6 × 6) superstructure observed by LEED. For the "thick" films (>4 MLE), no more Moiré structure is observed by STM and LEED. However, triangular pits and islands (Fig. 2e) which are very similar to those observed on ZnO(0 0 0 1) single-crystal surfaces [16,17] appear.

Taken together, the LEED, AES, STM, and TPD results show that the "as-prepared" films first form ZnO(0 0 0 1) monolayer islands which coalesce until the film covers the entire metal substrate. The films then grow in a layer-by-layer mode. Upon increasing the thickness to above 4 MLE, the film surface is essentially the same as that of a ZnO(0 0 0 1) single crystal, although the surface termination has not yet been identified.

The ZnO films, characterized by LEED, AES, and CO TPD, were then examined in the CO oxidation reaction at near-atmospheric pressures at 450 K. The reactivity measurements were performed in an excess of oxygen (CO/O_2 = 1/5) in order to prevent any possible oxide reduction and film dewetting and also to compare with the previously studied FeO/Pt(1 1 1) films, which exhibited film dewetting under oxygen-lean conditions [18,19].

Fig. 3 shows CO_2 production rate as a function of the nominal film thickness measured *prior to* the reaction. It is therefore clear that the reaction exhibits a strong rate enhancement at sub-monolayer coverage. Interestingly, the 1 MLE film shows some activity, at least, it is higher than on pure Pt(1 1 1). As the thickness further increases, the rate gradually decreases such that the multilayer, "thick" ZnO films become almost inert under the conditions studied. Note also that the reaction kinetics observed for the most active ZnO films show no deactivation in time.

AES characterization of the spent catalysts did not reveal considerable changes in the film stoichiometry, although the samples were lightly contaminated with carbon, particularly at the sub-monolayer coverages. LEED patterns showed diffuse (1 × 1) spots of Pt(1 1 1) and ZnO(0 0 0 1), whereas the (6 × 6) superstructure spots vanished (Fig. 4). Subsequent TPD measurements showed a considerably higher CO uptake as compared to that of measured prior to the reaction, thus indicating film dewetting and concomitant Pt surface opening under the reaction conditions (Fig. S4).

The morphology of the catalysts was studied with STM *ex situ*. For this, the well-defined films were exposed to the same reaction conditions (10 mbar CO, 50 mbar O_2, He balance to 1 bar, 450 K) in a high-pressure cell for 10 min. The sample was evacuated and transferred into the analytical chamber via a gate valve and immediately scanned with STM at room temperature. The STM images of the "reacted" samples are displayed in Fig. 5. For the 0.25 MLE film, irregularly shaped islands of ~10 nm in lateral size are observed (Fig. 5a). The film coverage is reduced to ~0.18 ML (which is most likely overestimated due to the well-known tip convolution effect for small objects). Monolayer islands, which dominated the surface

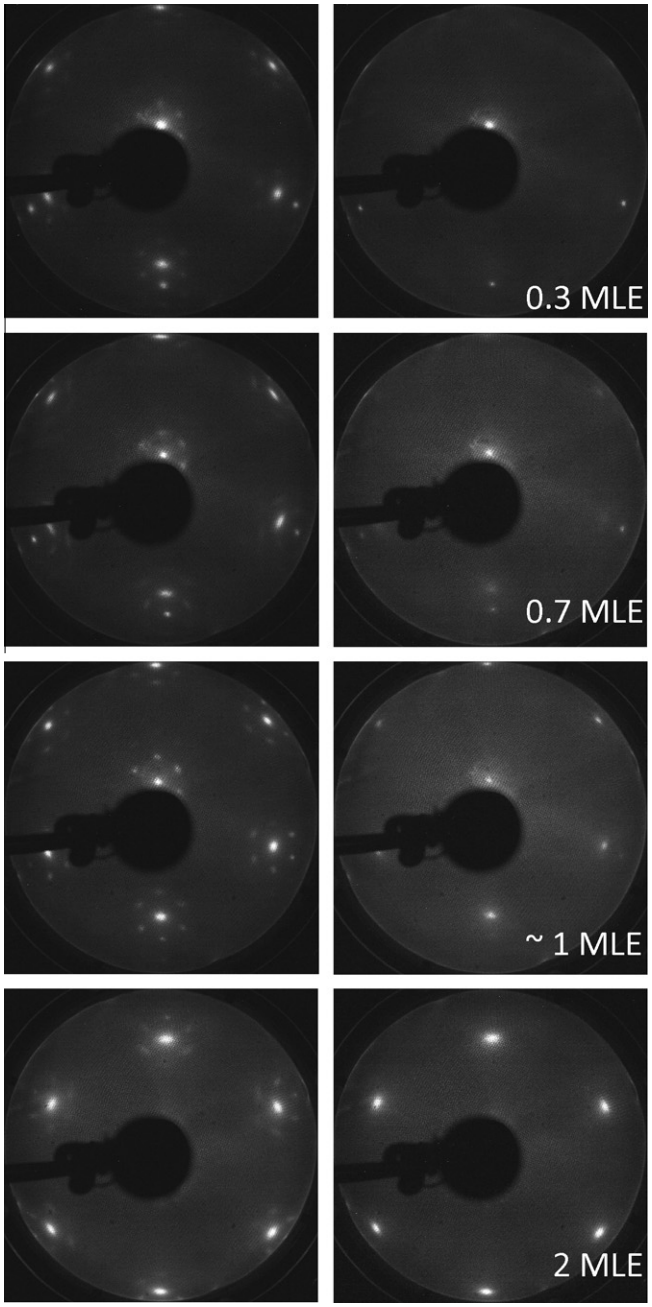

Fig. 4. LEED patterns (60 eV) of the ZnO films on Pt(1 1 1) before (left panel) and after (right panel) the reaction. The film thickness is indicated.

of the "as-prepared" film (see Fig. 2a), are no longer observed. Instead, the particles are all about 4 Å in height, thus indicating the formation of two-layers-thick (henceforth "bilayer") ZnO(0 0 0 1) islands. Similar behavior is observed for the 0.55 MLE film (Fig. 5b): The surface coverage decreases to ~0.32 ML, and the Pt(1 1 1) support is covered with small ~4 Å-high islands and their aggregates. Finally, the 1.2 MLE film dewets as well, thus forming a 0.75 ML covered "bilayer" film (Fig. 5d). For all films inspected, only small amounts of ZnO are found in the third layer. The long-range ordering via the Moiré (6×6) superstructure seen on the "as-prepared" films is hardly visible on the "reacted" films, in full agreement with the LEED data (Fig. 4).

The STM results show that the CO oxidation reaction on ZnO/Pt is accompanied by substantial structural transformations such that monolayer islands (and entire monolayer films) transform into the bilayer islands and their aggregates. Therefore, the Pt surface opening observed by CO uptake measurements of the spent catalyst reflects a higher stability of the bilayer structure at elevated pressures. The exact mechanism and the driving force for the observed structural changes are hard to envision on the basis of the existing results. Note, however, that bilayer ZnO islands were also stabilized on Pd(1 1 1) at increasing oxygen pressures used for oxidation at 550 K [10]. Interestingly, bilayer islands at sub-monolayer oxide coverages were also observed for CeO_2(1 1 1) films on Rh(1 1 1) [20] and Ru(0 0 0 1) [21].

The rate enhancement on the metal surfaces partially covered by oxide is commonly rationalized in terms of the reactions occurring at the oxide/metal boundary, which have been studied on the so-called inverse model catalysts (see, for example, Refs. [22–24]). Its perimeter also reaches a maximum at sub-monolayer coverage and goes to zero for a dense oxide film. In order to validate such a correlation, Fig. 6 shows the perimeter of the oxide islands, measured by STM on the "reacted" samples (see Fig. 5) and normalized to the surface area, as a function of the film nominal thickness measured prior to the reaction. This plot shows a fairly good correlation with reactivity data shown in Fig. 3, although the precise position of the maximum may deviate since the STM measurements were performed *ex situ* in another experimental setup.

In principle, the metal–oxide synergy effect may result either from oxygen spillover from oxide to Pt or from the formation of highly active sites at the metal/oxide boundary. Since ZnO is non-reducible oxide, the spillover mechanism seems to be unlikely.

Previously, a maximum in low-temperature CO oxidation in the sub-monolayer regime was reported by Hardacre et al. [25] for the CeO_x/Pt(1 1 1) system. The ceria coverage was measured by titration of bare Pt(1 1 1) with CO. Reactivity was measured in a high-pressure cell used as a batch reactor filled with ~10 Torr of stoichiometric (2:1) $CO + O_2$ mixture at a crystal temperature of 320–430 K. The authors found that the reaction rate increased between zero and 0.5 ML, after which it dropped almost to zero at 0.8–1.3 ML, but again increased steeply to a value which is much greater than that observed over the clean Pt(1 1 1) surface. It was suggested that for coverages below 1 ML, the reactivity is associated with the metal/oxide interface. The high reactivity of the thick ceria films, fully encapsulating Pt(1 1 1) (as judged by CO TPD *before* the reaction), was rationalized in terms of a proposal made by Frost [26] according to which electron transfer from a metal phase to an oxide phase reduces the enthalpy for oxygen vacancy formation in the oxide. However, the authors themselves argued that there was no absolute evidence of total encapsulation of the Pt crystal. In particular, the sample morphology *after* the reaction was undefined in this work. In principle, the initially dense oxide film could dewet under reaction conditions, ultimately forming ceria particles on Pt(1 1 1).

Nonetheless, the rate versus thickness plot observed for the CeO_{2-x}(1 1 1)/Pt(1 1 1) system is very different from that shown in Fig. 2 for ZnO(0 0 0 1)/Pt(1 1 1). While "thick" ceria films (~10 MLE) were much more active than Pt(1 1 1), the reactivity of ZnO(0 0 0 1)/Pt(1 1 1) dies away with increasing the film thickness. The difference may be related to the fact that ceria, well-known for its oxygen storage-release properties, readily provides weakly bound oxygen to react with CO, whereas ZnO does not.

Recently Sun et al. [27] performed density functional theory studies of the 3d transition-metal oxide (TMO) nano-islands on Pt(1 1 1) in low-temperature CO oxidation in order to identify the active sites at the TMO/Pt boundaries. A Pt-cation ensemble was proposed, where coordinatively unsaturated TMO cations exposed at the edges of oxide nano-islands are highly active for O_2 adsorption and dissociation, and less-reactive Pt binds modestly with dissociated O responsible for the facile CO oxidation. However, in all

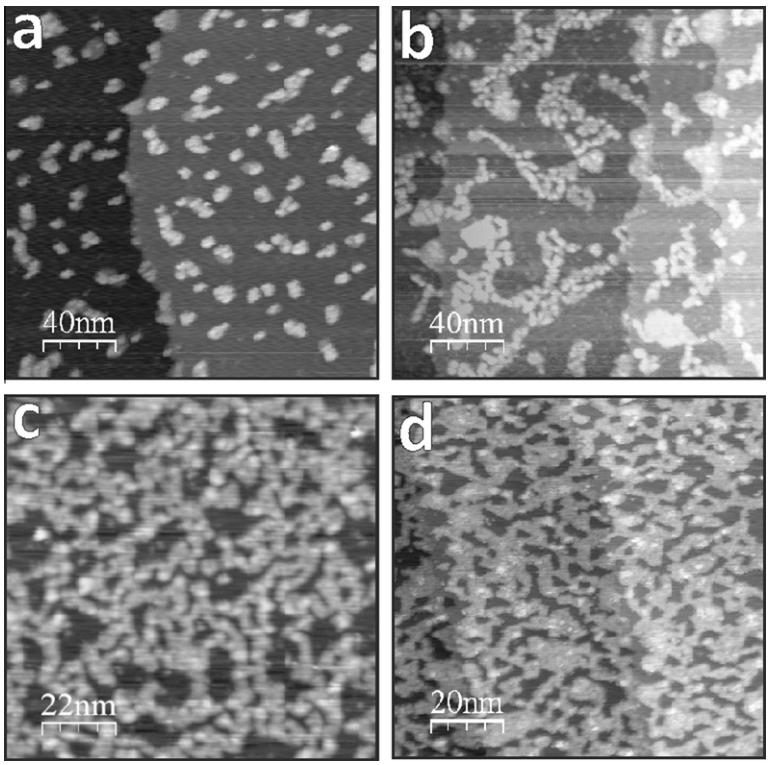

Fig. 5. STM images of the "reacted" ZnO films at 0.25 (a), 0.55 (b), 0.8 (c) and 1.2 MLE (d) film thicknesses.

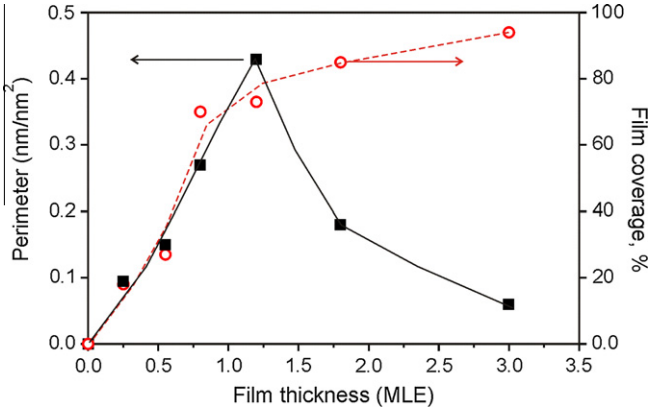

Fig. 6. The perimeter of oxide/metal boundary and the film coverage measured by STM on the "reacted" samples as a function of the nominal film thickness measured on the same samples before the reaction (10 mbar CO + 50 mbar O2, He balance; 450 K; 10 min).

these calculations, the TMO islands were only one monolayer in thickness, which is definitely not the case under technologically relevant conditions as shown here for ZnO(0001) and previously for FeO(111) on Pt(111) [3]. Therefore, our results provide more adequate structural models for TMO/metal "inverted" catalysts.

It is noteworthy that interfacial sites at oxide–metal interfaces have been long considered as active sites responsible for reactivity of oxide-supported metal catalysts. However, the proof has been exclusively based on density functional calculations of simplified models. Also, there were no experimental studies reported on model systems which could be directly correlated with the theoretical models. One of the very few studies where a direct comparison between calculations and experimental model studies has been carried out is for the above-mentioned FeO/Pt system. Very recently, Schlögl and his group have shown that a Pd/iron oxide powder catalyst also exhibits encapsulation of metal particles by an iron oxide overlayer that enhances reactivity.[28] In this case, the metal is completely covered with FeO, and therefore, there is no accessible oxide–metal interface to hold responsible for the increased reactivity. Control model system experiments with a fully covered film as opposed to a partially dewetted film have been carried out to confirm this statement.

In the present case, the corresponding experiments on fully covered ZnO films as well as on partially dewetted films have been performed, and here, the situation is opposite to the case of FeO/Pt. There are no directly comparable experiments available in the literature. Note, however, that Behrens et al. have recently presented evidence on ZnO/Cu methanol synthesis powder catalysts together with density functional calculations that it is the ZnO/Cu interface that is responsible for the high activity.[29] Again, there are no directly comparable experimental model studies available to validate or disprove this conclusion. The present data suggest that, indeed, the ZnO–metal interface may be responsible for reactivity of ZnO-based catalysts, although a direct verification is yet to be seen.

4. Conclusions

Well-ordered ZnO(0001) films on Pt(111) were studied in the CO oxidation reaction as a function of the film thickness and coverage. At low temperatures (450 K) and near-atmospheric pressures, CO_2 production is found to be much higher on the partially covered films than on the dense ZnO(0001) films and bare Pt(111). Under reaction conditions, monolayer structures transform into bilayer-thick islands, which dominate the surface of the active catalysts. The observed structure-reactivity relationships directly show that the oxide/metal boundary provides the active sites. The results provide a more adequate structural model than previously suggested for elucidating the reaction mechanism on the oxide/metal boundary at technologically relevant conditions.

Acknowledgments

BHL acknowledges the International Max Planck Research School "Complex surfaces in materials science". IMNG thanks the Alexander von Humboldt Foundation for a fellowship. MEM was a Fulbright Grantee in the Graduate Fellow Student Program 2011–2012. The work has been supported by Fonds der Chemischen Industrie, Deutsche Forschungsgemeinschaft, and Cluster of Excellence "UniCat".

Appendix A. Supplementary data

Supplementary data associated with this article can be found, in the online version, at http://dx.doi.org/10.1016/j.jcat.2013.02.018.

References

[1] S. Shaikhutdinov, H.-J. Freund, Annual Review of Physical Chemistry 63 (2012) 619–633.
[2] H.-J. Freund, G. Pacchioni, Chemical Society Reviews 37 (2008) 2224–2242.
[3] Y.-N. Sun, L. Giordano, J. Goniakowski, M. Lewandowski, Z.-H. Qin, C. Noguera, S. Shaikhutdinov, G. Pacchioni, H.-J. Freund, Angewandte Chemie – International Edition 49 (2010) 4418–4421.
[4] M. Lewandowski, Y.N. Sun, Z.H. Qin, S. Shaikhutdinov, H.J. Freund, Applied Catalysis A – General 391 (2011) 407–410.
[5] A. Hellman, S. Klacar, H. Grönbeck, Journal of the American Chemical Society 131 (2009) 16636–16637.
[6] F.F. Vol'kenshtein, Russian Chemical Reviews 35 (1966) 537.
[7] G.-M. Schwab, Advances in Catalysis 27 (1979) 1–22.
[8] A.A. Slinkin, E.A. Fedorovskaya, Russian Chemical Reviews 40 (1971) 860.
[9] C. Tusche, H.L. Meyerheim, J. Kirschner, Physical Review Letters 99 (2007) 026102.
[10] G. Weirum, G. Barcaro, A. Fortunelli, F. Weber, R. Schennach, S. Surnev, F.P. Netzer, The Journal of Physical Chemistry C 114 (2010) 15432–15439.
[11] C. Wöll, Progress in Surface Science 82 (2007) 55–120.
[12] E. Weiss, M. Folman, Journal of the Chemical Society, Faraday Transactions 1: Physical Chemistry in Condensed Phases 82 (1986) 2025–2041.
[13] W. Doerffler, K. Hauffe, Journal of Catalysis 3 (1964) 171–178.
[14] M. Kobayashi, B. Golman, T. Kanno, Journal of the Chemical Society, Faraday Transactions 91 (1995) 1391–1398.
[15] P. Esser, R. Feierabend, W. Göpel, Berichte der Bunsengesellschaft für physikalische Chemie 85 (1981) 447–455.
[16] O. Dulub, L.A. Boatner, U. Diebold, Surface Science 519 (2002) 201–217.
[17] O. Dulub, U. Diebold, G. Kresse, Physical Review Letters 90 (2003) 016102.
[18] Y.N. Sun, Z.H. Qin, M. Lewandowski, E. Carrasco, M. Sterrer, S. Shaikhutdinov, H.J. Freund, Journal of Catalysis 266 (2009) 359–368.
[19] Y.-N. Sun, Z.-H. Qin, M. Lewandowski, S. Kaya, S. Shaikhutdinov, H.-J. Freund, Catalysis Letters 126 (2008) 31–35.
[20] S. Eck, C. Castellarin-Cudia, S. Surnev, M.G. Ramsey, F.P. Netzer, Surface Science 520 (2002) 173–185.
[21] J.L. Lu, H.J. Gao, S. Shaikhutdinov, H.J. Freund, Surface Science 600 (2006) 5004–5010.
[22] J. Schoiswohl, S. Eck, M.G. Ramsey, J.N. Andersen, S. Surnev, F.P. Netzer, Surface Science 580 (2005) 122–136.
[23] K. Hayek, B. Jenewein, B. Klötzer, W. Reichl, Topics in Catalysis 14 (2000) 25–33.
[24] A.B. Boffa, C. Lin, A.T. Bell, G.A. Somorjai, Catalysis Letters 27 (1994) 243–249.
[25] C. Hardacre, R.M. Ormerod, R.M. Lambert, The Journal of Physical Chemistry 98 (1994) 10901–10905.
[26] J.C. Frost, Nature 334 (1988) 577–580.
[27] D. Sun, X.-K. Gu, R. Ouyang, H.-Y. Su, Q. Fu, X. Bao, W.-X. Li, The Journal of Physical Chemistry C 116 (2012) 7491–7498.
[28] H.-J. Freund, G. Meijer, M. Scheffler, R. Schlögl, M. Wolf, Angewandte Chemie International Edition 50 (2011) 10064–10094.
[29] M. Behrens et al., Science 336 (2012) 893–897.